Int J Theor Phys (2010) 49: 2723–2733
DOI 10.1007/s10773-010-0465-4

Quantum Computation and Entangled-State Generation Through Photon Emission and Absorption Processes in Separated Cavities

Hong-Fu Wang · Shou Zhang · Kyu-Hwang Yeon

Received: 8 June 2010 / Accepted: 11 August 2010 / Published online: 24 August 2010

Abstract We propose a scheme to implement a two-bit conditional quantum phase gate and generate a multi-atom cluster state and a two-atom three-dimensional entangled state based on photon emission and absorption processes. In the scheme, a Λ-type atom and a V-type atom are individually trapped in two spatially separated cavities connected by an optical fiber. By choosing the interaction time and the ratio of coupling parameters appropriately, the gate operation and entanglement generation can be determinately achieved. We also discuss the influence of photon Leakage on the fidelities of the gate and entanglement and show that the scheme is scalable and feasible in the experimental realization and further utilization.

Keywords Quantum phase gate · Cluster state · Three-dimensional entangled state · Optical fiber

1 Introduction

In recent years, quantum computation and quantum entangled state preparation are two very important research fields in quantum information science. Quantum computation, which employs the principle of coherent superposition, can solve certain problems much faster than on a conventional computer. It is well known that a universal quantum computer can be built from only a one-bit unitary gate and a two-bit conditional quantum phase gate. Such gates have been intensively investigated and implemented by using different physical systems,

H.-F. Wang (✉) · S. Zhang
Department of Physics, College of Science, Yanbian University, Yanji, Jilin 133002, People's Republic of China
e-mail: hfwang@ybu.edu.cn

S. Zhang
e-mail: szhang@ybu.edu.cn

K.-H. Yeon
Department of Physics & BK21 Program for Device Physics, College of Natural Science, Chungbuk National University, Cheongju, Chungbuk 361-763, Republic of Korea

such as cavity quantum electrodynamics (QED) system [1–3], linear optical system [4], ion trap system [5, 6], nuclear magnetic resonance (NMR) system [7], Josephson charge qubits in superconducting circuit [8], and so on. On the other hand, quantum entanglement is one of the most striking features of quantum mechanics. It not only gives the possibility for the testing of quantum mechanics against local hidden theory, but also holds the key of applications in quantum information processing such as quantum cryptography [9], quantum teleportation [10], and quantum dense coding [11, 12]. Many theoretical and experimental schemes have been proposed to generate quantum entangled states [13–24].

The implementation of conditional quantum phase gate and generation of quantum entangled state between two spatially separated subsystems are very useful for distributed quantum computation. In 1997 Pellizzari [25] first proposed a scheme for reliable quantum state transfer between two atoms via an optical fibre in the presence of decoherence based on performing an adiabatic passage through two cavities which remain in their respective vacuum states during the whole operation. By using the similar setup, Serafini et al. [26] proposed a scheme to realize highly reliable swap and entangling gates between two atoms in distant cavities coupled by an optical fiber. In this paper, motivated by the ideas in Refs. [25, 26], we propose a theoretical scheme for the implementation of a two-bit conditional quantum phase gate and the generation of entangled atomic states through photon emission and absorption processes in distant cavities. Two atoms, one is Λ-type and the other is V-type, individually interact with two spatially separated large detuning optical cavities connected by an optical fiber. We analyze the influence of photon Leakage on the fidelities of the gate and entanglement showing that the present scheme is robust with respect to the atomic spontaneous decay and photon leakage out of fiber due to the dispersive atom-field interaction and strong cavity-fiber coupling strength.

The rest of the paper is organized as follows: In Sect. 2, we describe the basic model used in this paper and derive the effective Hamiltonian of the system. In Sect. 3, we show how to implement a two-bit conditional quantum phase gate by choosing the interaction time and the ratio of the coupling parameters. In Sect. 4, we show how to generate a multi-atom cluster state and a three-dimensional entangled state. In Sect. 5, we analyze and discuss the influence of photon leakage of the cavities and fiber on the implementation of conditional quantum phase gate and the generation of three-dimensional entangled state. Finally, a conclusion is given in Sect. 6.

2 Model

As shown in Fig. 1(a), we consider a cavity-fiber-cavity system, which consists of two spatially separated cavities (A and B) connected by an optical fiber. Two atoms, whose levels are depicted by Fig. 1(b), are individually trapped in cavities A and B. In cavity A the atomic transitions $|e_S\rangle \leftrightarrow |g_L\rangle$ ($|e_S\rangle \leftrightarrow |g_R\rangle$) are coupled to the left-circularly (right-circularly) polarized cavity modes with the coherent coupling rates $\lambda_{A,L}$ ($\lambda_{A,R}$); the transition $|g_0\rangle \leftrightarrow |e_S\rangle$ is driven by a π-polarized classical field with the Rabi frequency Ω_A. In cavity B the atomic transitions $|e_L\rangle \leftrightarrow |g_S\rangle$ ($|e_R\rangle \leftrightarrow |g_S\rangle$) are coupled to the left-circularly (right-circularly) polarized cavity modes with the coherent coupling rates $\lambda_{B,L}$ ($\lambda_{B,R}$); the transitions $|g_L\rangle \leftrightarrow |e_L\rangle$ and $|g_R\rangle \leftrightarrow |e_R\rangle$ are driven by a π-polarized classical field with the Rabi frequency Ω_B. Under the dipole and rotating-wave approximation, the Hamiltonian of the system in the interaction picture is ($\hbar = 1$) [26, 27]

$$H_{\mathrm{I}} = H_{\mathrm{I}}^{A} + H_{\mathrm{I}}^{B} + H_{\mathrm{I}}^{F}, \tag{1}$$

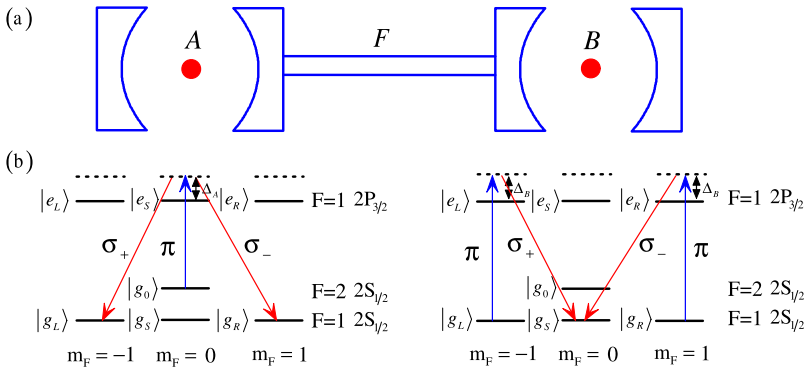

Fig. 1 (**a**) Schematic of cavity-fiber-cavity system. (**b**) Involved atomic levels and transitions in cavities A and B, respectively

where

$$
\begin{aligned}
H_{\mathrm{I}}^{A} &= -\Delta_A |e_S\rangle_A\langle e_S| + \Big(\Omega_A |e_S\rangle_A\langle g_0| + \sum_{j=L,R} \lambda_{A,j} a_{A,j} |e_S\rangle_A\langle g_j| + \mathrm{H.c.}\Big), \\
H_{\mathrm{I}}^{B} &= -\Delta_B (|e_L\rangle_B\langle e_L| + |e_R\rangle_B\langle e_R|) + \Big[\Omega_B (|e_L\rangle_B\langle g_L| + |e_R\rangle_B\langle g_R|) \\
&\quad + \sum_{j=L,R} \lambda_{B,j} a_{B,j} |e_j\rangle_B\langle g_S| + \mathrm{H.c.}\Big], \\
H_{\mathrm{I}}^{F} &= \sum_{j=L,R} \xi_j b_j (a_{A,j}^{\dagger} + a_{B,j}^{\dagger}) + \mathrm{H.c.},
\end{aligned}
\tag{2}
$$

where H_{I}^{i} $(i = A, B)$ and H_{I}^{F} (here we consider the case of short fiber limit $(2L\overline{v})/(2\pi C) \leq 1$, with L being the length of fiber and $\overline{v}$ being the decay rate of the cavity fields into a continuum of fiber modes, only resonant modes of the fiber interacts with the cavity modes.) denote the interaction Hamiltonian of atom-cavity and cavity-fiber, respectively; $a_{A/B,j}$ $(j = L, R)$ are the annihilation operators of the two circular polarizations $\sigma_{\pm}$, respectively; ξ_j and b_j $(j = L, R)$ are the cavity-fiber coupling constants and the annihilation operators for photons associating with the fiber corresponding to different circular polarization; Δ_A and Δ_B are the frequency detunings.

In the case of large-detuning conditions, i.e., $|\Delta_k| \gg |\Omega_k|, |\lambda_{k,l}|$ $(k = A, B;\ l = L, R)$, the excited states of atoms $|e_m\rangle$ $(m = L, S, R)$ are only virtually excited in the process of atom-cavity interaction. Therefore, by applying standard quantum optical techniques, the excited states can be eliminated adiabatically to obtain the effective Hamiltonian

$$
\begin{aligned}
H_{\mathrm{eff}} &= \sum_{j=L,R} \big[\zeta_{A,j}\big(a_{A,j}|g_0\rangle\langle g_j| + a_{A,j}^{\dagger}|g_j\rangle\langle g_0|\big) + \zeta_{B,j}\big(a_{B,j}|g_j\rangle\langle g_S| + a_{B,j}^{\dagger}|g_S\rangle\langle g_j|\big)\big] \\
&\quad + \Big[\sum_{j=L,R} \xi_j b_j \big(a_{A,j}^{\dagger} + a_{B,j}^{\dagger}\big) + \mathrm{H.c.}\Big],
\end{aligned}
\tag{3}
$$

where $\zeta_{n,k}=\frac{\lambda_{n,k}\Omega_n}{\Delta_n}$ $(n=A,B;\ k=L,R)$ are the effective Rabi frequencies. In the process of deriving effective Hamiltonian (3), we have safely neglected the terms of cavity- and laser-induced atomic level shifts, which can be compensated by using second lasers which couple corresponding atomic levels nonresonantly with additional levels farther up in the atomic level scheme [25].

3 Implementation of Conditional Quantum Phase Gate

In this section, we show how to implement a two-bit conditional quantum phase gate by using the model mentioned in Sect. 2. The quantum information is stored in the states $|g_S\rangle$ and $|g_0\rangle$, i.e., the qubits are encoded by $|g_S\rangle\equiv|0\rangle$, $|g_0\rangle\equiv|1\rangle$. Assume that all the cavity modes are initially in the vacuum state $|0\rangle_A|0\rangle_B|0\rangle_F$. Under the Hamiltonian (3), the states $|g_S\rangle_A|g_S\rangle_B$ and $|g_S\rangle_A|g_0\rangle_B$ do not evolve with time since $H_{\rm eff}|g_S\rangle_A|g_S\rangle_B|0\rangle_A|0\rangle_B|0\rangle_F=H_{\rm eff}|g_S\rangle_A|g_0\rangle_B|0\rangle_A|0\rangle_B|0\rangle_F=0$. The time evolutions of the states $|g_0\rangle_A|g_0\rangle_B|0\rangle_A|0\rangle_B|0\rangle_F$ and $|g_0\rangle_A|g_S\rangle_B|0\rangle_A|0\rangle_B|0\rangle_F$ are governed by the Schrödinger equation

$$i\frac{\partial}{\partial t}|\psi(t)\rangle=H_{\rm eff}|\psi(t)\rangle. \tag{4}$$

If the state of the system is initially in the state $|g_0\rangle_A|g_0\rangle_B|0\rangle_A|0\rangle_B|0\rangle_F$, after time t, this state will evolve to

$$\begin{aligned}&|g_0\rangle_A|g_0\rangle_B|0\rangle_A|0\rangle_B|0\rangle_F\\&\quad\to a_1(t)|g_0\rangle_A|g_0\rangle_B|0\rangle_A|0\rangle_B|0\rangle_F+a_2(t)|g_L\rangle_A|g_0\rangle_B|1_L\rangle_A|0\rangle_B|0\rangle_F\\&\qquad+a_3(t)|g_L\rangle_A|g_0\rangle_B|0\rangle_A|0\rangle_B|1_L\rangle_F+a_4(t)|g_L\rangle_A|g_0\rangle_B|0\rangle_A|1_L\rangle_B|0\rangle_F\\&\qquad+a_5(t)|g_R\rangle_A|g_0\rangle_B|1_R\rangle_A|0\rangle_B|0\rangle_F+a_6(t)|g_R\rangle_A|g_0\rangle_B|0\rangle_A|0\rangle_B|1_R\rangle_F\\&\qquad+a_7(t)|g_R\rangle_A|g_0\rangle_B|0\rangle_A|1_R\rangle_B|0\rangle_F,\end{aligned} \tag{5}$$

where $|1_{L(R)}\rangle$ denotes either a photon number state with one left- and/or right-circularly polarized photon. If the state of the system is initially in the state $|g_0\rangle_A|g_S\rangle_B|0\rangle_A|0\rangle_B|0\rangle_F$, the state will evolve to

$$\begin{aligned}&|g_0\rangle_A|g_S\rangle_B|0\rangle_A|0\rangle_B|0\rangle_F\\&\quad\to b_1(t)|g_0\rangle_A|g_S\rangle_B|0\rangle_A|0\rangle_B|0\rangle_F+b_2(t)|g_L\rangle_A|g_S\rangle_B|1_L\rangle_A|0\rangle_B|0\rangle_F\\&\qquad+b_3(t)|g_L\rangle_A|g_S\rangle_B|0\rangle_A|0\rangle_B|1_L\rangle_F+b_4(t)|g_L\rangle_A|g_S\rangle_B|0\rangle_A|1_L\rangle_B|0\rangle_F\\&\qquad+b_5(t)|g_L\rangle_A|g_L\rangle_B|0\rangle_A|0\rangle_B|0\rangle_F+b_6(t)|g_R\rangle_A|g_S\rangle_B|1_R\rangle_A|0\rangle_B|0\rangle_F\\&\qquad+b_7(t)|g_R\rangle_A|g_S\rangle_B|0\rangle_A|0\rangle_B|1_R\rangle_F+b_8(t)|g_R\rangle_A|g_S\rangle_B|0\rangle_A|1_R\rangle_B|0\rangle_F\\&\qquad+b_9(t)|g_R\rangle_A|g_R\rangle_B|0\rangle_A|0\rangle_B|0\rangle_F.\end{aligned} \tag{6}$$

For simplicity, we set $\Delta_A=\Delta_B=\Delta$, $\xi_L=\xi_R=\xi$, $\lambda_{A,L}=\lambda_{A,R}=\lambda_{B,L}=\lambda_{B,R}=\lambda$, $\Omega_A=\Omega=\frac{\Omega_B}{\sqrt{2}}$. In this way we have $\zeta_{A,L}=\zeta_{A,R}=\zeta=\frac{\zeta_{B,L}}{\sqrt{2}}=\frac{\zeta_{B,R}}{\sqrt{2}}$. Substituting (5) and (6) into (4), we get

$$
\begin{aligned}
a_1(t) &= \frac{1}{2}\big[\cosh(\mu t)+\cosh(\nu t)\big]+\frac{\xi^2-\zeta^2}{2\sqrt{\xi^4+\zeta^4}}\big[\cosh(\mu t)-\cosh(\nu t)\big],\\
a_2(t) &= a_5(t)=\frac{i}{4\zeta}\big[\mu\sinh(\mu t)+\nu\sinh(\nu t)\big]+\frac{i(\xi^2-\zeta^2)}{4\zeta\sqrt{\xi^4+\zeta^4}}\big[\mu\sinh(\mu t)-\nu\sinh(\nu t)\big],\\
a_3(t) &= a_6(t)=\frac{\xi\zeta[\cosh(\nu t)-\cosh(\mu t)]}{2\sqrt{\xi^4+\zeta^4}},\\
a_4(t) &= a_7(t)=-\frac{i\xi^2\zeta}{2\sqrt{\xi^4+\zeta^4}}\left[\frac{\sinh(\nu t)}{\nu}-\frac{\sinh(\mu t)}{\mu}\right],
\end{aligned}
\tag{7}
$$

where $\mu=\sqrt{-\xi^2-\zeta^2+\sqrt{\xi^4+\zeta^4}}$ and $\nu=\sqrt{-\xi^2-\zeta^2-\sqrt{\xi^4+\zeta^4}}$. And

$$
\begin{aligned}
b_1(t) &= \frac{1}{2}\big[\cos(\sqrt{2}\zeta t)+1\big]+\frac{\zeta^2}{2(\xi^2+\zeta^2)}\big\{\cos\big[\sqrt{2\big(\xi^2+\zeta^2\big)}t\big]-1\big\},\\
b_2(t) &= b_6(t)=-\frac{i}{2\sqrt{2}}\left\{\sin(\sqrt{2}\zeta t)+\frac{\zeta}{\sqrt{\xi^2+\zeta^2}}\sin\big[\sqrt{2\big(\xi^2+\zeta^2\big)}t\big]\right\},\\
b_3(t) &= b_7(t)=\frac{\xi\zeta}{2(\xi^2+\zeta^2)}\big\{\cos\big[\sqrt{2\big(\xi^2+\zeta^2\big)}t\big]-1\big\},\\
b_4(t) &= b_8(t)=\frac{i}{2\sqrt{2}}\left\{\sin(\sqrt{2}\zeta t)-\frac{\zeta}{\sqrt{\xi^2+\zeta^2}}\sin\big[\sqrt{2\big(\xi^2+\zeta^2\big)}t\big]\right\},\\
b_5(t) &= b_9(t)=\frac{1}{2\sqrt{2}(\xi^2+\zeta^2)}\big\{\xi^2+\zeta^2\cos\big[\sqrt{2\big(\xi^2+\zeta^2\big)}t\big]-\big(\xi^2+\zeta^2\big)\cos(\sqrt{2}\zeta t)\big\}.
\end{aligned}
\tag{8}
$$

We notice that in (8), if choosing $\sqrt{2}\zeta t=2n\pi$ $(n=1,2,3,\ldots)$ and $\sqrt{\xi^2+\zeta^2}=\zeta\sqrt{1+\frac{\xi^2}{\zeta^2}}=m\zeta$ $(m=1,2,3,\ldots)$, then we have $b_1=1$ and $b_i=0$ $(i=2,3,\ldots,9)$. In this way, we obtain the form of the quantum phase gate in the computational subspace spanned by $\{|g_S\rangle_A|g_S\rangle_B,\ |g_S\rangle_A|g_0\rangle_B,\ |g_0\rangle_A|g_S\rangle_B,\ |g_0\rangle_A|g_0\rangle_B\}$, as given below:

$$
\begin{aligned}
|g_S\rangle_A|g_S\rangle_B &\longrightarrow |g_S\rangle_A|g_S\rangle_B,\\
|g_S\rangle_A|g_0\rangle_B &\longrightarrow |g_S\rangle_A|g_0\rangle_B,\\
|g_0\rangle_A|g_S\rangle_B &\longrightarrow |g_0\rangle_A|g_S\rangle_B,\\
|g_0\rangle_A|g_0\rangle_B &\longrightarrow -\alpha|g_0\rangle_A|g_0\rangle_B,
\end{aligned}
\tag{9}
$$

with

$$
\begin{aligned}
\alpha &= a_1(\sqrt{2}n\pi/\zeta)=-\frac{1}{2}\big[\cosh\big(\sqrt{2}n\mu'\pi\big)+\cosh\big(\sqrt{2}n\nu'\pi\big)\big]\\
&\quad+\frac{2-m^2}{2\sqrt{(m-1)^2+1}}\big[\cosh\big(\sqrt{2}n\mu'\pi\big)-\cosh\big(\sqrt{2}n\nu'\pi\big)\big],\\
\mu' &= \sqrt{-m^2+\sqrt{\big(m^2-1\big)^2+1}},\\
\nu' &= \sqrt{-m^2-\sqrt{\big(m^2-1\big)^2+1}}\quad (m,n=1,2,3,\ldots).
\end{aligned}
\tag{10}
$$

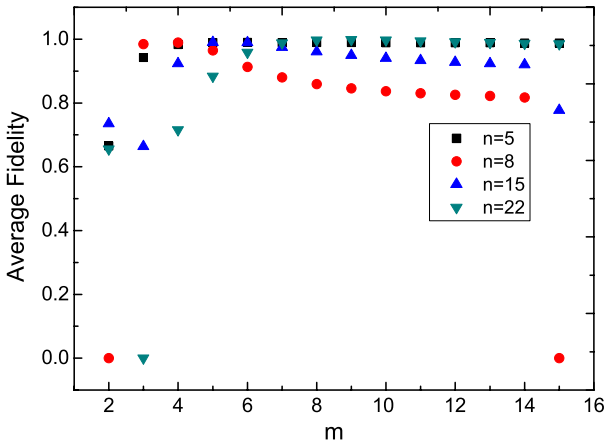

Fig. 2 The average fidelity of the conditional quantum phase gate. Here m and n are denoted by (10)

To qualify the performance of the conditional quantum phase gate, we introduce the gate fidelity defined as [28]

$$\mathcal{F}_{\mathrm{QPG}} = \overline{\langle \Psi_0 | U^{\dagger} \rho_t U | \Psi_0 \rangle}, \tag{11}$$

where the overline indicates average over all possible input states $|\Psi_0\rangle$, U is the ideal two-qubit conditional quantum phase gate, and $\rho_t = |\Psi_t\rangle\langle\Psi_t|$, with $|\Psi_t\rangle$ being the final state after the quantum phase gate operation in our scheme. Assume that the two atoms are initially in the general state $|\Psi_0\rangle = (\cos\theta_1|g_S\rangle_1 + \sin\theta_1|g_0\rangle_1) \otimes (\cos\theta_2|g_S\rangle_2 + \sin\theta_2|g_0\rangle_2) \otimes |0\rangle_A|0\rangle_B|0\rangle_F$, the ideal target state is $|\Psi_s\rangle = [\cos\theta_1|g_S\rangle_1 \otimes (\cos\theta_2|g_S\rangle_2 + \sin\theta_2|g_0\rangle_2) + \sin\theta_1|g_0\rangle_1 \otimes (\cos\theta_2|g_S\rangle_2 - \sin\theta_2|g_0\rangle_2)] \otimes |0\rangle_A|0\rangle_B|0\rangle_F$. Then the average fidelity of this quantum phase gate can be written as

$$\mathcal{F}_{\mathrm{QPG}} = \frac{1}{4\pi^2} \int_0^{2\pi} \mathrm{d}\theta_1 \int_0^{2\pi} \mathrm{d}\theta_2 |\langle \Psi_s | \Psi_t \rangle|^2. \tag{12}$$

To obtain an efficient quantum phase gate with high fidelity, we numerically calculate the average fidelity versus m when n is set to different values in Fig. 2. Through the calculation, we find that when we choose $\xi = \sqrt{35}\zeta$ ($m = 6$) and $t = \frac{5\sqrt{2}\pi}{\zeta}$ ($n = 5$), the quantum phase gate can be achieved with the fidelity of $\mathcal{F}_{\mathrm{QPG}} = 0.98983$ and the corresponding probabilistic amplitude of the state $|g_0\rangle_A|g_0\rangle_B$ is -0.979547. The fidelity of this gate can further be increased to 0.99873 when choosing $\xi = \sqrt{80}\zeta$ ($m = 9$) and $t = \frac{22\sqrt{2}\pi}{\zeta}$ ($n = 22$). In this case, the corresponding amplitudes of probabilities are

$$\begin{aligned}
|g_S\rangle_A|g_S\rangle_B &\longrightarrow |g_S\rangle_A|g_S\rangle_B, \\
|g_S\rangle_A|g_0\rangle_B &\longrightarrow |g_S\rangle_A|g_0\rangle_B, \\
|g_0\rangle_A|g_S\rangle_B &\longrightarrow |g_0\rangle_A|g_S\rangle_B, \\
|g_0\rangle_A|g_0\rangle_B &\longrightarrow -0.99745|g_0\rangle_A|g_0\rangle_B.
\end{aligned} \tag{13}$$

For the other choices, we can also obtain a quantum phase gate with high fidelity (see Fig. 2 in detail).

4 Generation of Cluster State and Three-Dimensional Entangled State

To demonstrate the possible application of our quantum phase gate, in this section, we show how to generate a multi-atom cluster state in two spatially separated cavities. Furthermore, we also show how to generate a three-dimensional entangled state based on the model of implementing the quantum phase gate.

To generate a multi-atom cluster state, we prepare all the atoms whose level configuration is shown in Fig. 1(b) in the state

$$|\phi\rangle_0 = |+\rangle_1 \otimes |+\rangle_2 \otimes \cdots \otimes |+\rangle_N \tag{14}$$

where $|+\rangle_i = (|g_S\rangle_i + |g_0\rangle_i)/\sqrt{2}$. We firstly put atoms 1 and 2 in cavities A and B, after applying the quantum phase gate to atoms 1 and 2, atom 1 leaves cavity A and atom 3 enters cavity A. Repeating the application of the quantum phase gate between atoms j and $j+1$, we obtain a N-atom cluster state

$$\begin{aligned}|\phi\rangle_r = {} & \frac{1}{\sqrt{2^N}}(|g_S\rangle_1 + |g_0\rangle_1\sigma_2) \otimes (|g_S\rangle_2 + |g_0\rangle_2\sigma_3) \\ & \otimes \cdots \otimes (|g_S\rangle_{N-1} + |g_0\rangle_{N-1}\sigma_N) \otimes (|g_S\rangle_N + |g_0\rangle_N),\end{aligned} \tag{15}$$

where $\sigma_k = |g_S\rangle_k\langle g_S| - |g_0\rangle_k\langle g_0|$ $(k = 2, 3, \ldots, N)$.

We now continue to demonstrate the generation of three-dimensional entangled state of two atoms in two distant cavities. Initially, atoms 1 and 2 are prepared in the state

$$|\varphi\rangle_0 = \frac{1}{\sqrt{3}}(|g_S\rangle_1 + \sqrt{2}|g_0\rangle_1) \otimes |g_S\rangle_2 \tag{16}$$

and all the cavity modes are in the vacuum state $|0\rangle_A|0\rangle_B|0\rangle_F$. It is obvious that the state $|g_S\rangle_1|g_S\rangle_2|0\rangle_A|0\rangle_B|0\rangle_F$ does not evolve under the Hamiltonian (3) and the expression of the time evolution of the state $|g_0\rangle_1|g_S\rangle_2|0\rangle_A|0\rangle_B|0\rangle_F$ is denoted by (6). In (8), choosing $\sqrt{2}\zeta t = n'\pi$ $(n' = 1, 3, 5, \ldots)$ and $\sqrt{\xi^2 + \zeta^2} = m'\zeta$ $(m' = 2, 4, 6, \ldots)$, then we have $b_5 = b_9 = 1/\sqrt{2}$ and $b_1 = b_2 = b_3 = b_4 = 0$. In this way we obtain a three-dimensional entangled state of two atoms in the form as given below:

$$|\varphi\rangle_r = \frac{1}{\sqrt{3}}(|g_S\rangle_1|g_S\rangle_2 + |g_L\rangle_1|g_L\rangle_2 + |g_R\rangle_1|g_R\rangle_2), \tag{17}$$

with the success probability of 1.0. The fidelity of generating such a three-dimensional entangled state is given by

$$\mathcal{F}_{\mathrm{TES}} = \left|\langle 0_A, 0_B, 0_F|_r\langle\varphi|\Psi(t)\rangle\right|^2, \tag{18}$$

where $|\Psi(t)\rangle$ is the resulting state of the whole system and $|\varphi\rangle_r$ is denoted by (17). In Fig. 3, the fidelity $\mathcal{F}_{\mathrm{TES}}$ is plotted for the cases with different ratios between ξ and ζ.

5 Effect of Photon Leakage

In this section, we investigate the influence of photon leakage of the cavities and fiber on the implementation of conditional quantum phase gate and the generation of three-dimensional

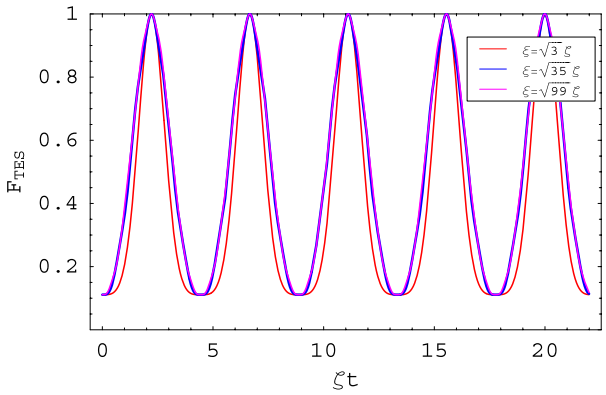

Fig. 3 The fidelity of generating a three-dimensional entangled state $|\varphi\rangle_r$ versus ζt

entangled state. The spontaneous decay of the atoms can be strongly suppressed due to the large atom-field detuning $|\Delta_k| \gg |\Omega_k|, |\lambda_{k,l}|$ $(k = A, B;\ l = L, R)$, so that it does not play a remarkable role in the dynamical evolution. The master equations for the density matrices of the whole system are expressed as

$$\begin{aligned}\dot{\rho}_o = &-i[H_{\text{eff}}, \rho_o] - \sum_{j=L,R} \frac{\kappa_{F,j}}{2}\left(b_j^\dagger b_j \rho_o - 2b_j \rho_o b_j^\dagger + \rho_o b_j^\dagger a_j\right) \\ &- \sum_{j=L,R} \frac{\kappa_{A,j}}{2}\left(a_{A,j}^\dagger a_{A,j} \rho_o - 2a_{A,j} \rho_o a_{A,j}^\dagger + \rho_o a_{A,j}^\dagger a_{A,j}\right) \\ &- \sum_{j=L,R} \frac{\kappa_{B,j}}{2}\left(a_{B,j}^\dagger a_{B,j} \rho_o - 2a_{B,j} \rho_o a_{B,j}^\dagger + \rho_o a_{B,j}^\dagger a_{B,j}\right), \end{aligned} \tag{19}$$

where ρ_o are the density matrices of the whole system corresponding to the implementation of quantum phase gate (ρ_{QPG}) and the generation of three-dimensional entangled state (ρ_{TES}), H_{eff} is given by (3), $\kappa_{A,j}$, $\kappa_{B,j}$ and $\kappa_{F,j}$ denote the decay rates for photons in mode j of cavities A and B, and the fiber, respectively. For solving the master equation numerically, we set $\Delta_A = \Delta_B = \Delta$, $\xi_L = \xi_R = \xi$, $\lambda_{A,L} = \lambda_{A,R} = \lambda_{B,L} = \lambda_{B,R} = \lambda$, $\Omega_A = \Omega = \frac{\Omega_B}{\sqrt{2}}$, $\kappa_{F,L} = \kappa_{F,R} = \kappa_F$, $\kappa_{A,j} = \kappa_{B,j} = \kappa_C$. In this case, the fidelities of the quantum phase gate ($\mathcal{F}_{\text{QPG}}$) and the three-dimensional entangled state ($\mathcal{F}_{\text{TES}}$) are plotted in Figs. 4 and 5, respectively. We can see from Figs. 4 and 5 that the influence of fiber decay rate κ_F is smaller than that of cavity field decay rate κ_C, and in the meanwhile both the influences of the cavity field decay rate and the fiber decay rate on the fidelities $\mathcal{F}_{\text{QPG}}$ and $\mathcal{F}_{\text{TES}}$ are very small.

Before ending this section, we briefly discuss the experimental feasibility of our scheme. Based on recent experiments in realizing high-$\mathcal{Q}$ cavity and strong atom-cavity coupling, we can choose $\Delta = 10\lambda = 10\,\Omega$, $\lambda/2\pi = 800$ MHz, $\kappa_C/2\pi = 1.6$ MHz, and $\kappa_F/2\pi = 8.4$ MHz [29–32] as the basic system parameters of our scheme. As for the fiber coupling to the cavities, a perfect fiber-cavity coupling (with efficiency larger than 99.9%) can be realized by fiber-taper coupling to high-$\mathcal{Q}$ silica microspheres. On the other hand, to achieve the conditional quantum phase gate and the three-dimensional entangled-state generation, the conditions $\zeta t = \sqrt{2}n\pi$ $(n = 1, 2, 3, \ldots)$ and $\sqrt{\xi^2 + \zeta^2} = m\zeta$ $(m = 1, 2, 3, \ldots)$ $[\zeta t = n'\pi/\sqrt{2}$ $(n' = 1, 3, 5, \ldots)$ and $\sqrt{\xi^2 + \zeta^2} = m'\zeta$ $(m' = 2, 4, 6, \ldots)]$ should be satisfied. By choosing the interaction time and the ratio ξ/ζ appropriately, we can obtain the higher fidelities of the conditional quantum phase gate and the three-dimensional entangled-state. Therefore,

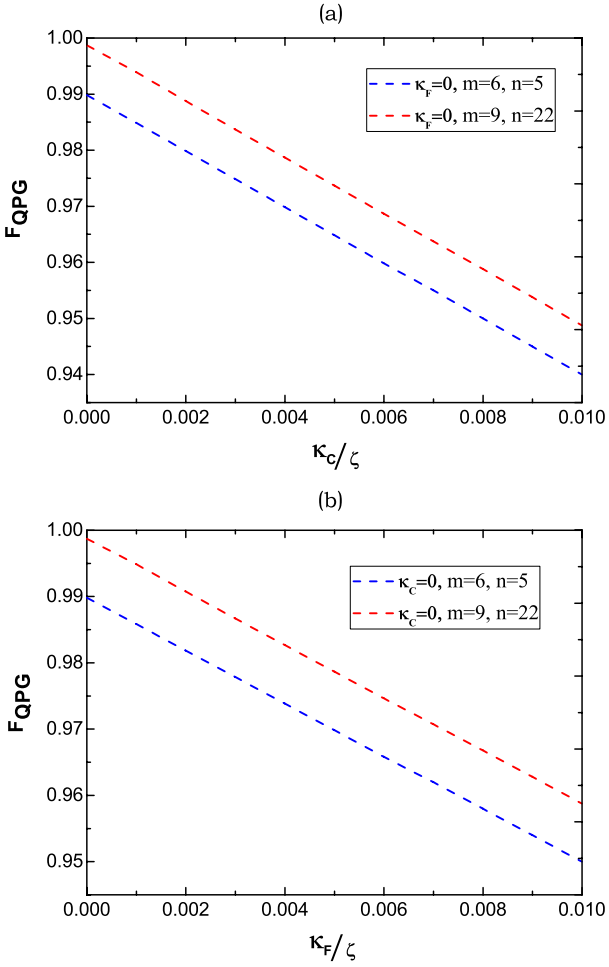

Fig. 4 Fidelities of implementing conditional quantum phase gate versus κ_C/ζ and κ_F/ζ, respectively. Here m and n are denoted by (10), i.e., $(m=6,\ n=5)$ corresponds to that $(\zeta t = 5\sqrt{2}\pi,\ \xi = \sqrt{35}\zeta)$ and $(m=9,\ n=22)$ corresponds to that $(\zeta t = 22\sqrt{2}\pi,\ \xi = \sqrt{80}\zeta)$

we believe that it is feasible with present techniques to realize quantum computation and three-dimensional entangled-state generation under consideration in this paper.

6 Conclusion

In conclusion, based on the photon emission and absorption processes, we have proposed a scheme to deterministically implement a two-bit conditional quantum phase gate and generate entangled states of spatially separated atoms. Through numerical calculation, we show that the proposed scheme is robust against atomic spontaneous decay and photon leakage out of the fiber because atomic excited states and the mode of the fiber are only virtually excited during the interaction processes. We also analyze the experimental feasibility of the present scheme and show that the gate operation and the entangled state generation can be reliably achieved with high fidelity. The experimental realization of the scheme would be useful step toward long-distance quantum communication, distributed quantum computation, and constructing remote quantum information processing networks.

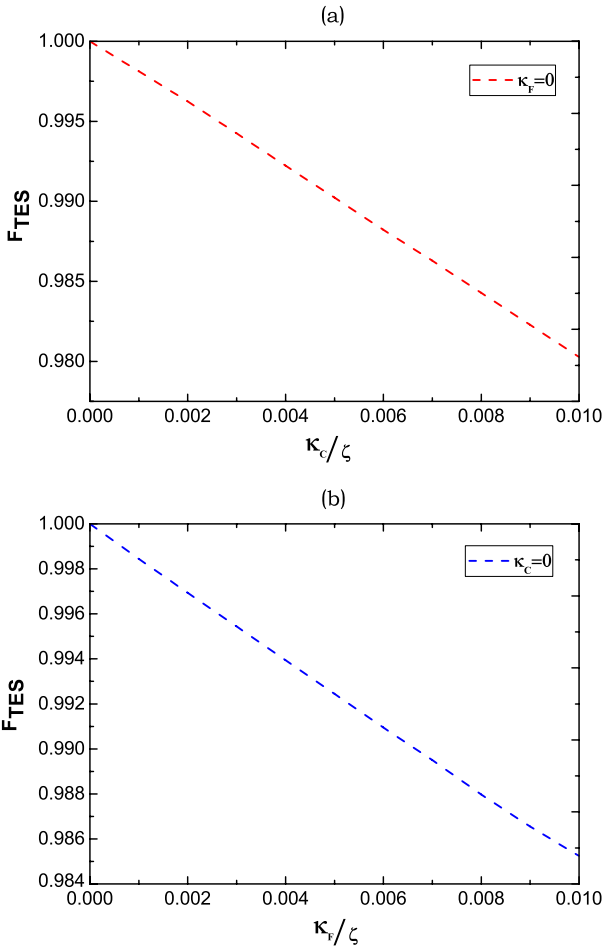

Fig. 5 Fidelities of generating the three-dimensional entangled state $|\varphi\rangle_r$ versus κ_C and κ_F, respectively. Here we have chosen $\zeta t = \pi/\sqrt{2}$, and $\xi = \sqrt{3}\zeta$

References

1. Turchette, Q.A., Hood, C.J., Lange, W., Mabuchi, H., Kimble, H.J.: Phys. Rev. Lett. **75**, 4710 (1995)
2. Rauschenbeutel, A., Nogues, G., Osnaghi, S., Bertet, P., Brune, M., Raimond, J.M., Haroche, S.: Phys. Rev. Lett. **83**, 5166 (1999)
3. Zou, X.B., Xiao, Y.F., Li, S.B., Yang, Y., Guo, G.C.: Phys. Rev. A **75**, 064301 (2007)
4. Zou, X.B., Zhang, S.L., Li, K., Guo, G.C.: Phys. Rev. A **75**, 034302 (2007)
5. Cirac, J.I., Zoller, P.: Phys. Rev. Lett. **74**, 4091 (1995)
6. Kielpinski, D., Monroe, C., Wineland, D.J.: Nature (London) **417**, 709 (2002)
7. Gershenfeld, N.A., Chuang, I.L.: Science **275**, 350 (1997)
8. Niskanen, A.O., Vartiainen, J.J., Salomaa, M.M.: Phys. Rev. Lett. **90**, 197901 (2003)
9. Ekert, A.K.: Phys. Rev. Lett. **67**, 661 (1991)
10. Bennett, C.H., Brassard, G., Crépeau, C., Jozsa, R., Peres, A., Wootters, W.K.: Phys. Rev. Lett. **70**, 1895 (1993)
11. Bennett, C.H., Wiesner, S.J.: Phys. Rev. Lett. **69**, 2881 (1992)
12. Bennett, C.H.: Phys. Rev. Lett. **68**, 3121 (1992)
13. Duan, L.M., Lukin, M.D., Cirac, J., Zoller, P.: Nature (London) **414**, 413 (2001)
14. Simon, C., Irvine, W.T.M.: Phys. Rev. Lett. **91**, 110405 (2003)
15. Zou, X.B., Pahlke, K., Mathis, W.: Phys. Rev. A **68**, 024302 (2003)
16. Deng, Z.J., Feng, M., Gao, K.L.: Phys. Rev. A **75**, 024302 (2007)

17. Tashima, T., Wakatsuki, T., Özdemir, S.K., Yamamoto, T., Koashi, M., Imoto, N.: Phys. Rev. Lett. **102**, 130502 (2009)
18. Wang, H.F., Zhang, S.: Phys. Rev. A **79**, 042336 (2009)
19. Bose, S., Knight, P.L., Plenio, M.B., Vedral, V.: Phys. Rev. Lett. **83**, 5158 (1999)
20. Wang, H.F., Zhang, S.: Eur. Phys. J. D **53**, 359 (2009)
21. Cabrillo, C., Cirac, J.I., Garcia-Fernandez, P., Zoller, P.: Phys. Rev. A **59**, 1025 (1999)
22. Zou, X.B., Pahlke, K., Mathis, W.: Phys. Rev. A **69**, 052314 (2004)
23. Zou, X.B., Pahlke, K., Mathis, W.: Phys. Rev. A **66**, 044302 (2002)
24. Feng, X.L., Zhang, Z.M., Li, X.D., Gong, S.Q., Xu, Z.Z.: Phys. Rev. Lett. **90**, 217902 (2003)
25. Pellizzari, T.: Phys. Rev. Lett. **79**, 5242 (1997)
26. Serafini, A., Mancini, S., Bose, S.: Phys. Rev. Lett. **96**, 010503 (2006)
27. Wu, Y., Saldana, J., Zhu, Y.: Phys. Rev. A **67**, 013811 (2003)
28. Poyatos, J.F., Cirac, J.I., Zoller, P.: Phys. Rev. Lett. **78**, 390 (1997)
29. Vahala, K.J.: Nature (London) **421**, 925 (2003)
30. Vernooy, D.W., Ilchenko, V.S., Mabuchi, H., Streed, E.W., Kimble, H.J.: Opt. Lett. **23**, 247 (1998)
31. Buck, J.R., Kimble, H.J.: Phys. Rev. A **67**, 033806 (2003)
32. Spillane, S.M., Kippenberg, T.J., Vahala, K.J., Goh, K.W., Wilcut, E., Kimble, H.J.: Phys. Rev. A **71**, 013817 (2005)